
SparseForge: Efficient Semi-Structured LLM Sparsification via Annealing of Hessian-Guided Soft-Mask

Hanzuo Liu^{†‡} Chaofan Lin[†] Weixuan Sun[‡] Yulong Wang[‡]
Rayying[‡] Key[‡] Mingyu Gao[†]

[†]Tsinghua University [‡]Tencent

{lh24@mails., lcf24@mails., gaomy}@tsinghua.edu.cn

<https://github.com/tsinghua-ideal/SparseForge>

Abstract

Semi-structured sparsity provides a practical path to accelerate large language models (LLMs) with native hardware support, but post-training semi-structured pruning often suffers from substantial quality degradation due to strong structural coupling. Existing methods rely on large-scale sparse retraining to recover accuracy, resulting in high computational cost.

We propose SparseForge, a post-training framework that improves recovery efficiency by directly optimizing the sparsity mask rather than scaling up retraining tokens. SparseForge combines Hessian-aware importance estimation with progressive annealing of soft masks into hardware-executable structured sparsity, enabling stable and efficient sparse recovery. On LLaMA-2-7B under 2:4 sparsity, SparseForge achieves 57.27% average zero-shot accuracy with only **5B** retraining tokens, surpassing the dense model’s 56.43% accuracy and approaching the 57.52% result of a state-of-the-art method using **40B** tokens. Such improvements on the accuracy-efficiency trade-off from SparseForge are shown to be consistent across model families.

1 Introduction

Semi-structured sparsity stands out as one of the few sparsity paradigms that deliver both meaningful compression and tangible hardware acceleration for large language models (LLMs). In particular, patterns such as 2:4 sparsity are natively supported by modern NVIDIA Sparse Tensor Core pipelines, making them attractive for practical deployment [22]. However, in post-training LLM sparsification, achieving high accuracy under such structured constraints typically requires substantial retraining, leading to a nontrivial trade-off between performance and training cost.

Existing post-training pruning methods often rely on computing importance scores for weights followed by hard projection to sparse structures [9, 13, 14, 28]. While effective in simpler settings, this paradigm becomes brittle under semi-structured constraints, where pruning decisions are no longer independent. Instead, weights compete within each constrained group, and premature hard decisions can remove weights that are individually important but suboptimal under imperfect scoring. As a result, these approaches either suffer from noticeable accuracy degradation or require large amounts of retraining to recover performance.

We argue that this challenge is fundamentally rooted in *how sparsity masks are learned*. Rather than committing to a discrete mask prematurely, semi-structured sparsification should treat the mask as a continuous and optimizable variable, allowing the model to explore structured alternatives before making irreversible pruning decisions. More importantly, we argue that improving mask optimization

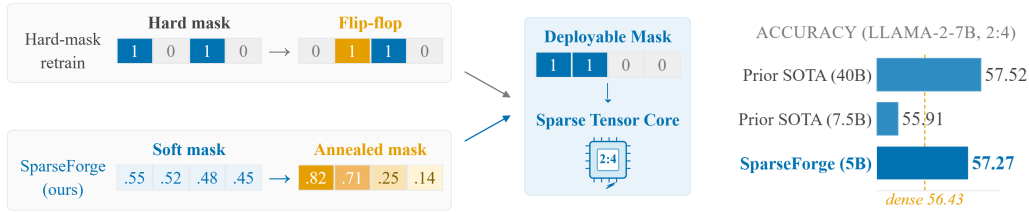


Figure 1: **(a)** Compared with hard-mask retraining, SparseForge explicitly optimizes a soft mask and progressively anneals it into a deployable binary 2:4 mask. **(b)** On LLaMA-2-7B under 2:4 sparsity, SparseForge achieves 57.27% average zero-shot accuracy with 5B retraining tokens, approaching the 57.52% result of the stronger 40B-token prior SOTA variant [14] while using about $8\times$ fewer training tokens.

quality can reduce reliance on large-scale retraining, offering a more efficient path to sparse recovery. Adopting a continuous mask formulation, however, introduces a new challenge: at inference time the mask must be an exact, hardware-executable binary pattern, creating a gap between the learned soft mask and its deployment-time hard counterpart. In practice, naive soft-mask approaches often lead to performance degradation when the mask is binarized, due to insufficient separation between mask values.

Based on this perspective, we propose **SparseForge** (Figure 1), a post-training framework for semi-structured sparsification that leverages *Hessian-aware importance* guideline to derive a *soft mask*, and progressively hardens it by gradually shaping from continuous exploratory values into deployable binary sparse structures. SparseForge improves mask optimization quality via three key techniques: (1) continuous soft-mask optimization for stable structured exploration; (2) Hessian-aware importance estimation to better capture deletion sensitivity under grouped competition; and (3) a progressive annealing mechanism that gradually aligns soft masks with hardware-executable binary patterns. With improved mask quality, SparseForge largely reduces retraining tokens and hence achieves efficient sparse recovery. The main contributions of this work are as follows:

- We identify that under semi-structured constraints, sparse recovery is bottlenecked more by mask quality than by retraining scale. This insight motivates us to prioritize optimizing the mask itself and to keep it soft during retraining, which leads to the proposed *mask annealing* pipeline that efficiently navigates the soft-to-hard transition.
- We present SparseForge, a post-training framework for semi-structured sparsification that explicitly optimizes the mask itself. SparseForge features a Hessian-aware mask annealing algorithm, which smoothly trains the soft mask towards a hardware-executable binary pattern.
- We show that SparseForge attains accuracy on par with both the dense model and state-of-the-art sparse methods with *remarkably fewer retraining tokens* (e.g., 5B vs. 40B on LLaMA-2-7B). Extensive ablations further verify the contribution of its key components.

2 Related Work

Hardware-aligned sparsity patterns. Structured sparsity has long been pursued as a practical route to efficient neural network acceleration, since regular sparse patterns are far easier for hardware and kernels to exploit than irregular ones [10, 18, 19, 21, 31]. Early work explored filter-, channel-, and block-level pruning for real execution benefits. More recently, semi-structured patterns such as 2:4 sparsity have drawn significant attention due to native GPU support [22]. While offering clear deployment gains, such patterns impose tightly coupled local constraints—selecting exactly N survivors within each group of M (in practice $N=2$, $M=4$, i.e., 2:4 sparsity)—which makes their accuracy impact more substantial than flexible, unstructured cases.

Unstructured sparsification for LLMs. A large body of recent work studies post-training sparsification for LLMs in the unstructured setting. Building on classical magnitude-based pruning [11], representative methods such as SparseGPT [9] and Wanda [28] estimate weight importance via

approximate second-order information or activation statistics, removing parameters with little or no retraining. OWL [34] further shows that outlier-weighted, layerwise sparsity allocation is critical for pushing LLMs to high sparsity. BESA [32] introduces a blockwise sparsity allocation strategy, but its goal is still not hardware-aligned semi-structured execution. However, unstructured sparsity does not translate into efficient execution on current accelerators, so it does not resolve the deployment problem targeted by hardware-aligned patterns.

Structured sparsification for LLMs. Recent efforts therefore turn to structured or semi-structured sparsification for LLMs. MaskLLM [8] cast $N:M$ mask selection as a learnable discrete distribution optimized via Gumbel-Softmax sampling on large-scale corpora, while AST [13] followed a dense-to-sparse adaptive sparse training scheme that progressively annealed the weights toward the 2:4 pattern. More recently, CAST [14] relaxed the hard 2:4 constraint into a continuous, differentiable form so that masks could be optimized jointly with weights. These works show that better mask optimization can substantially narrow the gap of hardware-executable sparse models, yet they all rely on training over a large number of tokens for the mask to converge to a high-quality solution. Our work instead targets *recovery efficiency* by improving mask optimization quality itself, attaining strong recovery with considerably fewer retraining tokens.

3 Motivation

3.1 Rethinking the Bottleneck of Sparse Recovery: Mask Quality over Retraining Scale

As discussed in §2, previous methods such as CAST [14] preserve quality by scaling retraining tokens, which yields gains but with poor efficiency. Observations from CAST show that even with substantial retraining, accuracy is still governed by the selected sparse pattern, implying that *mask quality, rather than retraining scale alone, is the key bottleneck*. We instead choose to directly improve the quality of mask optimization along three axes: (1) keeping the mask soft long enough to avoid brittle early hard decisions, (2) using Hessian-aware importance to resolve intra-group competition, and (3) progressively annealing the mask into the final hardware-executable 2:4 pattern.

3.2 Soft Masks are Necessary under Grouped Semi-structured Constraints

Under semi-structured constraints such as 2:4 sparsity, pruning is no longer an element-wise decision but a grouped selection problem in which weights compete within each constrained block. Committing to a binary mask too early therefore locks the optimizer into a suboptimal sparse subspace before intra-group importance is sufficiently resolved. This effect is also reflected empirically in Figure 3(a): on the 7-task zero-shot benchmark, SparseForge achieves 59.20% mean accuracy, outperforming the hard-mask-style AST baseline at 58.62% [13]. This supports the need to *keep the mask soft* during optimization.

However, a soft mask must eventually be converted into a deployable binary (0/1) form. Combining the two sides, we propose a pipeline that we call *mask annealing* in this paper: first, we optimize the mask in a soft, continuous state to allow extensive exploration, analogous to heating metal into a malleable condition (**Heating**); then, we binarize the mask into the hardware-ready pattern, analogous to cooling it into a fixed shape (**Quenching**).

3.3 Insights to Implement Efficient Mask Annealing

With mask annealing, we appear to achieve the best of both worlds: the exploration flexibility of a soft mask and the deployment readiness of a hard mask. Yet, translating this idea into practice requires several key insights, which we detail below.

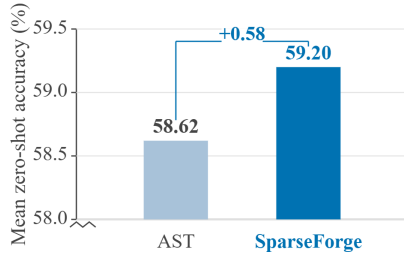


Figure 2: Soft masks improve sparse recovery: compared with the hard-mask-style AST baseline, our soft-mask-style SparseForge improves the mean zero-shot accuracy on the 7-task benchmark from 58.62% to 59.20%, supporting the need for soft mask optimization.

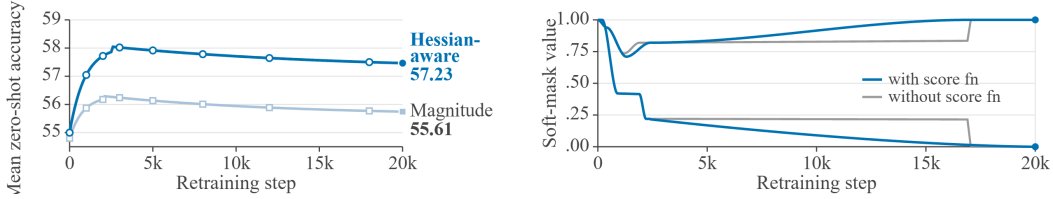


Figure 3: **(a)** Hessian-aware importance provides a better survival signal: replacing it with magnitude-based scoring drops mean zero-shot accuracy from 57.23% to 55.61%. **(b)** Soft masks must also be progressively hardened toward a deployable 2:4 pattern: score structural hardening pushes the top-2 and bottom-2 entries in each group towards 1 and 0, respectively; without such hardening, the mask remains far from binary, leading to a larger soft-to-hard gap at final projection.

(I1) Using second-order Hessian-aware loss signal. Even with a soft mask, the optimizer still needs to decide which entries should survive within each constrained group. A useful intuition comes from the local loss change incurred by removing a weight:

$$\Delta L = L(w_i = 0) - L(w_i) \approx \frac{\partial L}{\partial w_i}(-w_i) + \frac{1}{2} \frac{\partial^2 L}{\partial w_i^2} w_i^2$$

Near a converged solution, the first-order gradient term is typically negligible, so removal sensitivity is dominated by the local curvature term. Under grouped competition, magnitude alone is therefore often insufficient to determine which entries should be preserved. Figure 3(a) directly supports this point: using magnitude-based scoring to replace Hessian-aware importance would drop the mean zero-shot accuracy from 57.23% to 55.61%. This is also consistent with classical second-order pruning criteria [12, 17, 27] and modern LLM pruning methods such as SparseGPT [9].

(I2) The quenching process needs to be progressive. Under 2:4 sparsity, the two surviving entries in each group should approach 1, while the two pruned ones should approach 0. If many mask values remain in the middle of $[0, 1]$ in the late stages during training, the final quenching step must abruptly binarize them, causing a large projection error. This motivates us to optimize soft mask towards a near-binary structured solution during the heating stage, rather than relying on a late hard projection alone in the quenching stage. As in Figure 3(b), with a score function explicitly designed to encourage the mask toward a near-binary state, retraining steadily pushes the entries toward 0/1.

4 Methodology

Building on the insights from §3, we design **SparseForge**, a LLM sparsification framework that efficiently implements the mask annealing pipeline. Figure 4 provides an overview. In §4.1, we present the overall retraining loop of the heating stage, describing how the soft mask is optimized alongside model weights. §4.2 then addresses (I1) by detailing our second-order mask update rule, while §4.3 tackles (I2) and explains how progressive quenching bridges the soft-to-hard gap.

4.1 Dual-track Retraining Loop in the Heating Stage

During the heating stage, SparseForge jointly optimizes the model weights and the soft mask in a unified retraining loop. The weight update follows the paradigm established by prior sparse-training methods such as AST and CAST [13, 14]. Given a linear layer

$$Z = XW^T, \quad X \in \mathbb{R}^{N \times C}, \quad W \in \mathbb{R}^{D \times C}, \quad Z \in \mathbb{R}^{N \times D},$$

a sparse mask $m \in \{0, 1\}^{D \times C} \cap \mathcal{M}$ is applied in the forward pass by writing $\tilde{W} = m \odot W$, where \mathcal{M} is the semi-structured feasible set (e.g., 2:4 or block-16). The sparse forward pass, optionally equipped with a sparse low-rank branch (SLoRB) [13], is

$$\hat{Y} = X(\tilde{W}^T + P^T B^T), \quad (1)$$

where P is the fixed projection and B is a learnable low-rank parameter used to compensate for capacity lost during pruning. Our retraining objective builds upon prior work and introduces a structure-aware guidance term that facilitates progressive quenching:

$$\mathcal{L} = \lambda_{\text{task}} \mathcal{L}_{\text{task}} + \lambda_{\text{KL}} \mathcal{L}_{\text{KL}} + \lambda_{\text{mid}} \mathcal{L}_{\text{mid}}, \quad (2)$$

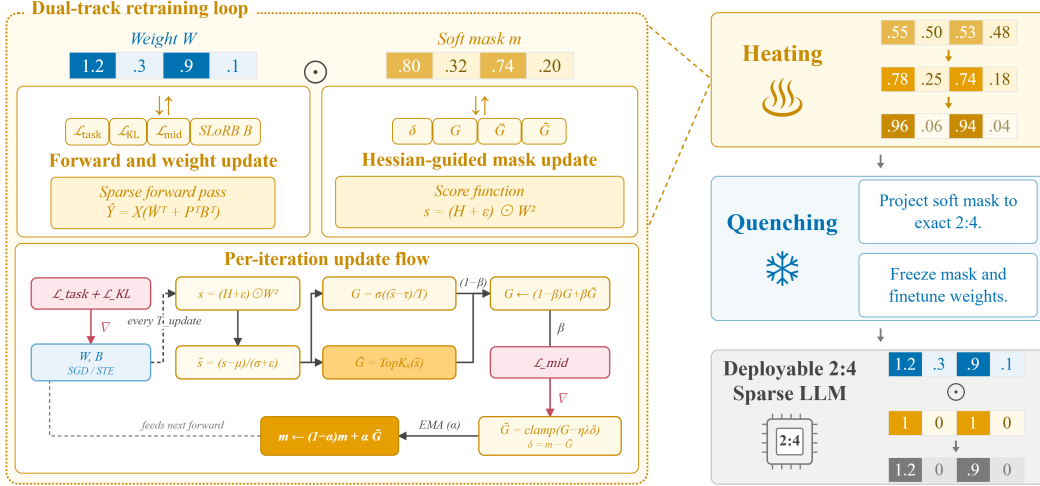


Figure 4: **Overview of SparseForge.** We first co-optimize the weights and the explicit learnable soft mask in a dual-track retraining loop (§4.1) in the heating stage, where the mask is updated with a Hessian-guided signal (§4.2). Then we progressively binarize the mask to a hard, deployable form in the quenching stage (§4.3).

where $\mathcal{L}_{\text{task}}$ and \mathcal{L}_{KL} inherit the standard task and distillation losses from prior work, and \mathcal{L}_{mid} extends the objective with a binary-preference regularizer that we design for the mask (§4.3).

Besides weight optimization, SparseForge performs explicit soft-mask learning. In prior works, masks are typically treated as hard selections derived from one-shot importance scores or updated through discrete re-selection steps, rather than being continuously optimized as learnable variables. SparseForge instead separates mask learning from weight adaptation and makes the soft mask the central object of optimization.

Specifically, we optimize a continuous mask $m \in [0, 1]^{D \times C}$ during retraining and only project it to a hardware-executable binary pattern at the end. Within the same unified loop, the optimization proceeds along two interleaved tracks: the weights W and the low-rank B follow the previous paradigm, updated by the loss at every step, while the soft mask m is updated by its own dedicated learning rule (§4.2) only every T_{update} steps. This decoupled schedule confines sparsification entirely to the mask space, where optimization remains more stable under grouped semi-structured constraints. We briefly sketch this *dual-track retraining loop* in Algorithm 1. The following sections elaborate the details.

4.2 Hessian-Guided Soft-Mask Update

Following (I1) (§3.3), we derive the survival signal for mask updates from a *Hessian-aware* criterion, which yields the classic OBD-style importance score [17]:

$$s = (H + \epsilon) \odot W^2, \quad s \in \mathbb{R}^{D \times C},$$

where s_{ij} measures the Hessian-aware pruning sensitivity of weight W_{ij} , $H \in \mathbb{R}^{D \times C}$ denotes an approximate Hessian diagonal reshaped to the weight matrix, and ϵ is a small stabilizer.

Since explicitly forming the Hessian is prohibitively expensive for LLMs, we estimate its diagonal with a Hutchinson-style stochastic estimator [15]:

$$\mathbb{E}[(Hv) \odot v] = \text{diag}(H), \quad v \sim \text{Rademacher}(\pm 1),$$

and maintain an exponential moving average of $(Hv) \odot v$ in practice.

To respect the final semi-structured constraint while keeping the mask continuous, we turn s into a soft group-wise gate rather than directly projecting it onto the feasible set. For an $N:M$ pattern, let $\text{Groups}(M)$ denote the collection of non-overlapping groups, each containing M mask entries along the structured sparsity dimension. For a group \mathcal{G} , $s_{\mathcal{G}}$ denotes the restriction of the score matrix s

Algorithm 1 SparseForge’s Dual-track Retraining Loop

Require: Dense weights W , semi-structured constraint \mathcal{M} , training data \mathcal{D} , mask update duration

- 1: Initialize soft mask $m \leftarrow \mathbf{1}$; initialize temperature $T \leftarrow T_0$ and structural-mix factor $\beta \leftarrow 0$
 - 2: Initialize optional SLoRB branch (P, B)
 - 3: **for** $t = 1$ to T_{\max} **do**
 - 4: Sample batch $(X, Y) \sim \mathcal{D}$
 - 5: Compute sparse forward pass with current soft mask m
 - 6: Update W (via STE) and B using $\lambda_{\text{task}}\mathcal{L}_{\text{task}} + \lambda_{\text{KL}}\mathcal{L}_{\text{KL}}$ $\{\mathcal{L}_{\text{mid}}$ enters through (4), not autograd}
 - 7: **if** $t \bmod T_{\text{update}} = 0$ **then**
 - 8: Compute importance score $s = (H + \epsilon) \odot W^2$; standardize to \tilde{s}
 - 9: Synthesize soft gate $G = \sigma((\tilde{s} - \tau)/T)$ with group-wise threshold τ , and hard target $\bar{G} = \text{TopK}_N(\tilde{s})$ on \mathcal{M}
 - 10: Blend in structure: $\tilde{G} \leftarrow (1 - \beta)G + \beta\bar{G}$
 - 11: Inject mid-penalty: $\tilde{G} \leftarrow \text{clamp}(G - \eta_{\text{pen}}\lambda_{\text{mid}}(m - \bar{G}), 0, 1)$
 - 12: Update soft mask: $m \leftarrow (1 - \alpha) \cdot m + \alpha \cdot \tilde{G}$
 - 13: Anneal schedules: $T \leftarrow \gamma T$; advance $\beta, \lambda_{\text{mid}}$
 - 14: **end if**
 - 15: **end for**
 - 16: **return** Near-hard mask m and the trained model
-

to the entries in \mathcal{G} . We first standardize the scores layer-wise so that the soft threshold has a stable physical scale, $\tilde{s} \leftarrow (s - \mu_s)/(\sigma_s + \epsilon)$, and then define, within each group, a soft gate and its hard top- N counterpart:

$$G_{\mathcal{G}} = \sigma\left(\frac{\tilde{s}_{\mathcal{G}} - \tau_{\mathcal{G}}}{T}\right), \quad \bar{G}_{\mathcal{G}} = \text{TopK}_N(\tilde{s}_{\mathcal{G}}), \quad \forall \mathcal{G} \in \text{Groups}(M), \quad (3)$$

where $\tau_{\mathcal{G}}$ is the N -th largest entry of $\tilde{s}_{\mathcal{G}}$, σ is the sigmoid, and $T > 0$ is a temperature. The soft gate G already encodes the N:M competition: the N largest entries in each group sit above 0.5 and the remaining $M - N$ sit below, with the decisiveness controlled by T . The hard counterpart $\bar{G} \in \{0, 1\}^{D \times C}$ is kept on the side as a curvature-guided structured target that we will mix into G progressively (§4.3).

Directly overwriting the soft mask with \bar{G} would destroy mask continuity and reintroduce premature hard-projection instability. We therefore use G only as an update direction, and push G toward it through the mid-penalty residual $\delta = m - \bar{G}$:

$$\tilde{G} = \text{clamp}(G - \eta_{\text{pen}}\lambda_{\text{mid}}\delta, 0, 1), \quad (4)$$

so that entries that the structured target wants to keep ($\bar{G}_{ij} = 1$) but the current mask has dropped (m_{ij} small) are nudged up, and vice versa. This is precisely the gradient of the binary-preference regularizer \mathcal{L}_{mid} (§4.3) evaluated against the structured target, and it is the only channel through which \mathcal{L}_{mid} influences the mask. Finally, we update the soft mask with an exponential moving average:

$$m \leftarrow (1 - \alpha) \cdot m + \alpha \cdot \tilde{G}. \quad (5)$$

This rule preserves soft-mask continuity while moving the mask toward entries that are important under the Hessian-aware loss signal and already compatible with the final N:M structure.

4.3 Progressive Soft-to-Hard Mask Quenching

(I2) implies that an abrupt projection from soft to binary mask is harmful. We therefore introduce *progressive quenching*, a strategy that incorporates structure-aware regularization and penalty terms throughout the heating stage, encouraging the mask to progressively approach a near-binary configuration before the final hardening step.

First, we introduce a binary-preference regularizer that penalizes ambiguous mask values:

$$\mathcal{L}_{\text{mid}} = \frac{1}{|m|} \sum_{i,j} m_{ij}(1 - m_{ij}).$$

This term is maximized at $m_{ij} = 0.5$ and minimized at $m_{ij} \in \{0, 1\}$. We anneal its weight λ_{mid} during training, keeping the binary preference weak during early exploration and progressively strengthening it as the mask approaches the final deployment stage.

Second, to inject structure awareness during training, we progressively blend the soft gate G from (3) with its Hessian-guided structured target \bar{G} before the mid-penalty injection of (4):

$$G \leftarrow (1 - \beta)G + \beta\bar{G}, \quad \beta : 0 \rightarrow 1.$$

We schedule β with a smooth-step (cubic Hermite) curve so that the update gradually shifts from soft exploration to structured hardening without a discontinuity in the gradient of the schedule itself. In parallel, we geometrically anneal the sigmoid temperature in (3), $T \leftarrow \gamma T$ with $\gamma \in (0, 1)$ applied at every mask-update step, so that the soft threshold sharpens monotonically as retraining proceeds. Among the three handles, the interpolation controlled by β is the primary driver: it continuously morphs the gate from the soft, exploratory G into the hard, group-structured target \bar{G} , while T sharpens the decisiveness of G in sync with this interpolation, and λ_{mid} adds a mild element-wise pressure that pushes any residual mid-range values in m toward $\{0, 1\}$. Consequently, the mask approaches a near-binary state while also aligning with the correct top- N pattern within each group.

Once the soft mask is sufficiently separated, the final quenching step interpolates between the soft mask and its hard version:

$$m_{\text{eff}} = x m + (1 - x) \mathbf{1}[m > \theta],$$

where x is annealed linearly from 1 to 0 over a dedicated hardening window. Once x reaches 0, we apply the final structured projection, freeze the binary mask, and run a short finetuning stage to absorb the remaining projection error.

5 Experiments

5.1 Experimental Setup

Models. We evaluate SparseForge on a diverse set of pretrained language models spanning different architectures and scales, including GPT-2 [24], OPT [36], LLaMA-2 [29], Qwen3 [33], and DeepSeek-MoE [6]. The evaluated model sizes range from 124M to 16B parameters, covering both dense transformer models and mixture-of-experts (MoE) architectures.

Hardware setting. All experiments are conducted on a cluster of 32 NVIDIA L20A GPUs. Training is implemented with distributed data parallelism. For LLaMA-2-7B, the full SparseForge training with 5B tokens requires approximately 50 GPU hours. Unless otherwise stated, all experiments target 2:4 semi-structured sparsity, i.e., 50% sparsity within every group of four weights. This sparsity pattern is directly supported by modern sparse Tensor Core hardware [22], making it a practically relevant deployment setting.

Training setup. For LLaMA-2-7B, we perform sparse retraining on Dolmino-mix-1124 [1, 23], following the data configuration adopted in recent continual pretraining and sparse recovery studies. For all other models, we use the C4 corpus [7, 25]. Unless otherwise specified, we use a total retraining budget of approximately 5B tokens for LLaMA-2-7B and 1.25B tokens for other models, substantially smaller than prior retraining-based methods such as AST [13] and CAST [14]. Unless otherwise specified, each SparseForge configuration is run with three random seeds. We report the mean performance across the three runs.

Table 1: Compact cross-model summary under 2:4 semi-structured sparsity. We report mean zero-shot accuracy (%) for the dense model, SparseForge, and their difference. Detailed task-level results are provided in Appendix Table 4.

Metric	GPT2-M	GPT2-L	GPT2-XL	OPT-2.7B	Qwen3-1.7B	Qwen3-8B	Qwen3-14B	DeepSeek-MoE
Dense	40.97	42.76	45.49	47.76	56.51	65.73	68.36	59.54
SparseForge	40.31	42.10	44.34	46.67	53.33	63.31	65.44	58.57
Diff	-0.66	-0.66	-1.15	-1.09	-3.18	-2.42	-2.93	-0.97

Table 2: Comparison with prior semi-structured sparsification methods on LLaMA-2-7B under 2:4 sparsity. Best results among *sparse methods* are highlighted in **bold**. For dense and SparseForge rows, we report our own re-evaluation results under the current `lm-evaluation-harness` setup; prior baseline numbers are taken from the corresponding original papers unless otherwise noted. [†] denotes a continual-training variant using a substantially larger retraining token budget.

Method	Pattern	Tokens	HellaS.	RACE	PIQA	WinoG.	ARC-e	ARC-c	OBQA	Average	Wiki PPL
Dense	Dense	2T	57.18	39.52	78.07	69.06	76.26	43.52	31.40	56.43	5.12
CAST [†]	2:4	40B	56.13	40.86	77.58	69.53	77.78	47.18	33.60	57.52	5.21
Wanda	2:4	×	41.05	35.02	70.78	62.67	61.99	27.56	22.80	45.98	11.29
SparseGPT	2:4	×	43.36	36.84	71.38	63.69	62.84	29.18	22.80	47.16	10.42
MaskLLM	2:4	2B	50.91	40.77	74.92	64.48	69.57	36.00	28.00	52.09	6.72
Naive Retrain	2:4	10B	53.90	38.28	76.61	68.27	75.21	41.21	29.60	54.73	5.78
SR-STE	2:4	10B	54.02	39.02	76.88	68.35	75.58	41.46	29.60	54.99	5.74
AST	2:4	7.5B	54.66	–	–	67.87	73.61	39.93	28.60	–	–
AST + SLoRB	2:4	7.5B	55.24	–	–	68.48	74.91	41.11	29.40	–	–
CAST	2:4	7.5B	54.50	40.48	77.09	68.27	76.52	43.68	30.80	55.91	5.58
SparseForge (ours)	2:4	1.25B	52.95	41.15	75.46	69.14	76.35	43.86	32.80	55.96	6.24
SparseForge [†] (ours)	2:4	5B	54.42	41.63	76.88	69.69	77.95	45.31	35.00	57.27	6.09

Evaluation metrics. We report WikiText-2 perplexity (PPL) and zero-shot accuracy on downstream tasks evaluated with `lm-evaluation-harness` [2]. For the cross-model comparison in Table 1, we use a benchmark suite that is consistent across model families and remains aligned with the reporting protocol of recent semi-structured sparsification work. This suite includes ARC-Challenge and ARC-Easy [5], BoolQ [4], HellaSwag [35], OpenBookQA [20], RTE [30], and WinoGrande [26].

For the detailed LLaMA-2-7B comparison in Table 2, we follow the benchmark configuration of CAST [14], adding RACE [16] and PIQA [3] to the above suite. We report mean accuracy over the corresponding task set in each table.

5.2 Results Across Model Families

To facilitate consistent comparison across architectures while staying aligned with recent semi-structured sparsification practice, we summarize the cross-model results in Table 1, while detailed task-level results are deferred to Appendix Table 4. SparseForge preserves model quality across diverse architectures and scales: although degradation varies across families, the drops in mean accuracy remain moderate in most cases, showing that continuous mask optimization with progressive quenching is a robust recipe for semi-structured sparsification beyond a single model family.

5.3 Comparison with Prior Methods on LLaMA-2-7B

We compare SparseForge with representative post-training and retraining-based semi-structured sparsification methods, including SparseGPT [9], Wanda [28], MaskLLM [8], AST [13], and CAST [14], under aligned 2:4 sparsity.

As shown in Table 2 and Figure 5, SparseForge achieves 57.27% average accuracy using only 5B retraining tokens, outperforming the 7.5B-token CAST result (55.91%) and approaching the stronger 40B-token continual-training CAST variant (57.52%) with roughly 8× fewer retraining tokens. This indicates that improved mask optimization and structure-aware tempering can substantially reduce the retraining required for high-quality semi-structured sparse recovery.

5.4 Ablation Studies

We conduct a full ablation of SparseForge on LLaMA-2-7B under 2:4 sparsity, using C4 [7, 25] as the default retraining corpus with 1.25B retraining tokens (20k steps). Table 3 studies the effects of retraining data, training budget, importance criterion, SLoRB, teacher scale, and distillation.

Several trends are clear. First, retraining data quality matters substantially: replacing C4 with Dolmino-mix-1124 improves mean accuracy from 57.23% to 59.22% and also lowers WikiText-2 perplexity. Second, SparseForge remains relatively token-efficient: halving the budget from 20k to 10k steps reduces mean accuracy by only 1.34%. Third, Hessian-aware importance is important for resolving intra-group competition: replacing it with magnitude-based scoring lowers mean accuracy by 1.62% and worsens perplexity. Finally, the remaining components also make nontrivial

Table 3: Full ablation on LLaMA-2-7B under 2:4 sparsity. Unless otherwise noted, variants are trained on C4 with 1.25B retraining tokens (20k steps). We report WikiText-2 perplexity, mean zero-shot accuracy, and the difference against the full SparseForge configuration.

Variant	Steps / Tokens	Wiki PPL	Mean Acc.	Diff vs Full
Dense	2T	5.1983	59.71%	+2.48%
SparseForge (full)	20k / 1.25B	6.3823	57.23%	–
SparseForge (dolmino)	20k / 1.25B	6.1037	59.22%	+1.99%
SparseForge w/ 10k steps	10k / 0.625B	6.4755	55.89%	-1.34%
SparseForge w/ magnitude	20k / 1.25B	6.5275	55.61%	-1.62%
SparseForge w/o SLoRB	20k / 1.25B	6.3617	55.04%	-2.19%
SparseForge w/ larger teacher (13B)	20k / 1.25B	6.6089	54.87%	-2.36%
SparseForge w/o distillation	20k / 1.25B	6.6594	55.72%	-1.51%

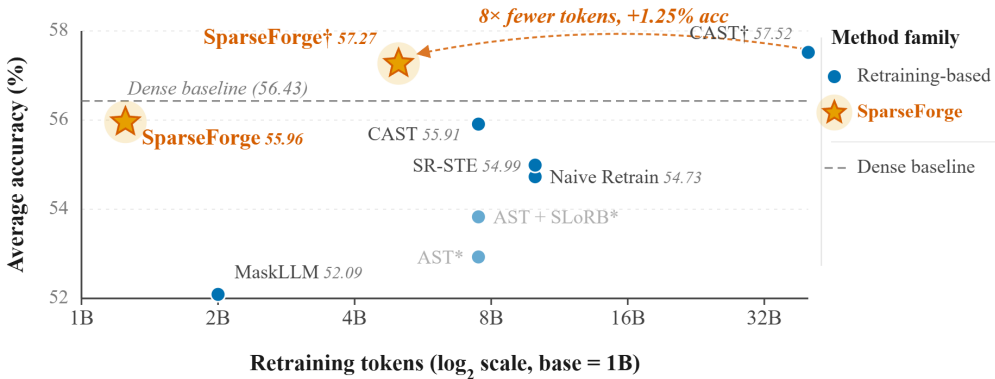


Figure 5: Accuracy vs. retraining tokens on LLaMA-2-7B (2:4 sparsity, log-scale). SparseForge matches the 40B-token CAST[†] with $\sim 8\times$ fewer tokens. AST/AST+SLoRB (semi-transparent) report only a 5-task mean.

contributions: removing SLoRB causes the largest drop among these auxiliary ablations (-2.19%), while removing distillation (-1.51%) or replacing the teacher with a larger 13B model (-2.36%) also degrades recovery. Overall, these results support the view that SparseForge benefits from both better mask optimization and careful training design, rather than from retraining scale alone.

6 Conclusion

We introduced **SparseForge**, a post-training framework for semi-structured sparsification that follows a mask-annealing pipeline: SparseForge explicitly learns and progressively quenches the sparsity mask toward a deployable 2:4 pattern, driven by a dual-track retraining loop that jointly updates weights and the soft mask under a Hessian-guided structured target. Our results suggest that under grouped semi-structured constraints, sparse recovery is governed more by mask quality than by retraining scale alone. By combining explicit soft-mask optimization, Hessian-guided structured targets, and progressive quenching within this dual-track loop, SparseForge achieves strong sparse recovery across model families and a favorable accuracy–efficiency trade-off under semi-structured sparsity, matching or surpassing prior state-of-the-art recovery while using substantially fewer retraining tokens. More broadly, these findings highlight mask-centric optimization as a promising direction for hardware-aligned sparse LLM compression.

References

- [1] Allen Institute for AI. allenai/dolmino-mix-1124. <https://huggingface.co/datasets/allenai/dolmino-mix-1124>, 2024. Hugging Face dataset card, accessed: 2026-04-30.
- [2] Stella Biderman, Hailey Schoelkopf, Lintang Sutawika, Leo Gao, Jonathan Tow, Baber Abbasi, Alham Fikri Aji, Pawan Sasanka Ammanamanchi, Sid Black, Jordan Clive, Anthony DiPofi, Julen Etxaniz, Benjamin Fattori, Jessica Zosa Forde, Charles Foster, Mimansa Jaiswal, Wilson Y. Lee, Haonan Li, Charles Lovering, Niklas Muennighoff, Ellie Pavlick, Jason Phang, Aviya Skowron, Samson Tan, Xiangru Tang, Kevin Wang, Genta Indra Winata, Franccois Yvon, and Andy Zou. Lessons from the trenches on reproducible evaluation of language models. *ArXiv*, abs/2405.14782, 2024. URL <https://api.semanticscholar.org/CorpusID:269982020>.
- [3] Yonatan Bisk, Rowan Zellers, Ronan Le Bras, Jianfeng Gao, and Yejin Choi. Piqa: Reasoning about physical commonsense in natural language. In *AAAI Conference on Artificial Intelligence*, 2019. URL <https://api.semanticscholar.org/CorpusID:208290939>.
- [4] Christopher Clark, Kenton Lee, Ming-Wei Chang, Tom Kwiatkowski, Michael Collins, and Kristina Toutanova. Boolq: Exploring the surprising difficulty of natural yes/no questions. *ArXiv*, abs/1905.10044, 2019. URL <https://api.semanticscholar.org/CorpusID:165163607>.
- [5] Peter Clark, Isaac Cowhey, Oren Etzioni, Tushar Khot, Ashish Sabharwal, Carissa Schoenick, and Oyvind Tafjord. Think you have solved question answering? try arc, the ai2 reasoning challenge. *ArXiv*, abs/1803.05457, 2018. URL <https://api.semanticscholar.org/CorpusID:3922816>.
- [6] Damai Dai, Chengqi Deng, Chenggang Zhao, Runxin Xu, Huazuo Gao, Deli Chen, Jiashi Li, Wangding Zeng, Xingkai Yu, Yu Wu, Zhenda Xie, Y. K. Li, Panpan Huang, Fuli Luo, Chong Ruan, Zhifang Sui, and Wenfeng Liang. Deepseekmoe: Towards ultimate expert specialization in mixture-of-experts language models. In *Annual Meeting of the Association for Computational Linguistics*, 2024. URL <https://api.semanticscholar.org/CorpusID:266933338>.
- [7] Jesse Dodge, Ana Marasovic, Gabriel Ilharco, Dirk Groeneveld, Margaret Mitchell, Matt Gardner, and William Agnew. Documenting large webtext corpora: A case study on the colossal clean crawled corpus. In *Conference on Empirical Methods in Natural Language Processing*, 2021. URL <https://api.semanticscholar.org/CorpusID:237568724>.
- [8] Gongfan Fang, Hongxu Yin, Saurav Muralidharan, Greg Heinrich, Jeff Pool, Jan Kautz, Pavlo Molchanov, and Xinchao Wang. Maskllm: Learnable semi-structured sparsity for large language models. *ArXiv*, abs/2409.17481, 2024. URL <https://api.semanticscholar.org/CorpusID:272910976>.
- [9] Elias Frantar and Dan Alistarh. Sparsegpt: Massive language models can be accurately pruned in one-shot. *ArXiv*, abs/2301.00774, 2023. URL <https://api.semanticscholar.org/CorpusID:255372747>.
- [10] Trevor Gale, Erich Elsen, and Sara Hooker. The state of sparsity in deep neural networks. *ArXiv*, abs/1902.09574, 2019. URL <https://api.semanticscholar.org/CorpusID:67855585>.
- [11] Song Han, Jeff Pool, John Tran, and William J. Dally. Learning both weights and connections for efficient neural network. In *Neural Information Processing Systems*, 2015. URL <https://api.semanticscholar.org/CorpusID:2238772>.
- [12] Babak Hassibi and David G. Stork. Second order derivatives for network pruning: Optimal brain surgeon. In *Advances in Neural Information Processing Systems*, 1993.
- [13] Weiyu Huang, Guohao Jian, Yuezhou Hu, Jun Zhu, and Jianfei Chen. Pruning large language models with semi-structural adaptive sparse training. In *AAAI Conference on Artificial Intelligence*, 2024. URL <https://api.semanticscholar.org/CorpusID:271544038>.

- [14] Weiyu Huang, Yuezhou Hu, Jun Zhu, and Jianfei Chen. Cast: Continuous and differentiable semi-structured sparsity-aware training for large language models. *ArXiv*, abs/2509.25996, 2025. URL <https://api.semanticscholar.org/CorpusID:281682355>.
- [15] M.F. Hutchinson. A stochastic estimator of the trace of the influence matrix for laplacian smoothing splines. *Communications in Statistics - Simulation and Computation*, 19(2): 433–450, 1990. doi: 10.1080/03610919008812866. URL <https://doi.org/10.1080/03610919008812866>.
- [16] Guokun Lai, Qizhe Xie, Hanxiao Liu, Yiming Yang, and Eduard H. Hovy. Race: Large-scale reading comprehension dataset from examinations. *ArXiv*, abs/1704.04683, 2017. URL <https://api.semanticscholar.org/CorpusID:6826032>.
- [17] Yann LeCun, John S. Denker, and Sara A. Solla. Optimal brain damage. In *Advances in Neural Information Processing Systems*, 1990.
- [18] Hao Li, Asim Kadav, Igor Durdanovic, Hanan Samet, and Hans Peter Graf. Pruning filters for efficient convnets. *ArXiv*, abs/1608.08710, 2016. URL <https://api.semanticscholar.org/CorpusID:14089312>.
- [19] Zhuang Liu, Jianguo Li, Zhiqiang Shen, Gao Huang, Shoumeng Yan, and Changshui Zhang. Learning efficient convolutional networks through network slimming. *2017 IEEE International Conference on Computer Vision (ICCV)*, pages 2755–2763, 2017. URL <https://api.semanticscholar.org/CorpusID:5993328>.
- [20] Todor Mihaylov, Peter Clark, Tushar Khot, and Ashish Sabharwal. Can a suit of armor conduct electricity? a new dataset for open book question answering. In *Conference on Empirical Methods in Natural Language Processing*, 2018. URL <https://api.semanticscholar.org/CorpusID:52183757>.
- [21] Asit K. Mishra, Jorge Albericio Latorre, Jeff Pool, Darko Stosic, Dusan Stosic, Ganesh Venkatesh, Chong Yu, and Paulius Micikevicius. Accelerating sparse deep neural networks. *ArXiv*, abs/2104.08378, 2021. URL <https://api.semanticscholar.org/CorpusID:233296249>.
- [22] NVIDIA. Nvidia ampere architecture in-depth. <https://developer.nvidia.com/blog/nvidia-ampere-architecture-in-depth/>, 2020. Accessed: 2026-04-30.
- [23] Team OLMo, Pete Walsh, Luca Soldaini, Dirk Groeneveld, Kyle Lo, Shane Arora, Akshita Bhagia, Yuling Gu, Shengyi Huang, Matt Jordan, Nathan Lambert, Dustin Schwenk, Oyvind Tafjord, Taira Anderson, David Atkinson, Faeze Brahman, Christopher Clark, Pradeep Dasigi, Nouha Dziri, Michal Guerquin, Hamish Ivison, Pang Wei Koh, Jiacheng Liu, Saumya Malik, William Merrill, Lester James Validad Miranda, Jacob Daniel Morrison, Tyler C. Murray, Crystal Nam, Valentina Pyatkin, Aman Rangapur, Michael Schmitz, Sam Skjonsberg, David Wadden, Christopher Wilhelm, Michael Wilson, Luke S. Zettlemoyer, Ali Farhadi, Noah Smith, and Hanna Hajishirzi. 2 olmo 2 furious. *ArXiv*, abs/2501.00656, 2024. URL <https://api.semanticscholar.org/CorpusID:275213098>.
- [24] Alec Radford, Jeffrey Wu, Rewon Child, David Luan, Dario Amodei, and Ilya Sutskever. Language models are unsupervised multitask learners. Technical report, OpenAI, 2019. URL https://cdn.openai.com/better-language-models/language_models_are_unsupervised_multitask_learners.pdf.
- [25] Colin Raffel, Noam Shazeer, Adam Roberts, Katherine Lee, Sharan Narang, Michael Matena, Yanqi Zhou, Wei Li, and Peter J. Liu. Exploring the limits of transfer learning with a unified text-to-text transformer. *J. Mach. Learn. Res.*, 21:140:1–140:67, 2019. URL <https://api.semanticscholar.org/CorpusID:204838007>.
- [26] Keisuke Sakaguchi, Ronan Le Bras, Chandra Bhagavatula, and Yejin Choi. Winogrande. *Communications of the ACM*, 64:99 – 106, 2019. URL <https://api.semanticscholar.org/CorpusID:198893658>.

- [27] Sidak Pal Singh and Dan Alistarh. Woodfisher: Efficient second-order approximations for model compression. *ArXiv*, abs/2004.14340, 2020. URL <https://api.semanticscholar.org/CorpusID:216641895>.
- [28] Mingjie Sun, Zhuang Liu, Anna Bair, and J. Zico Kolter. A simple and effective pruning approach for large language models. *ArXiv*, abs/2306.11695, 2023. URL <https://api.semanticscholar.org/CorpusID:259203115>.
- [29] Hugo Touvron, Louis Martin, Kevin R. Stone, Peter Albert, Amjad Almahairi, Yasmine Babaei, Niko Ilay Bashlykov, Soumya Batra, Prajjwal Bhargava, Shruti Bhosale, Daniel M. Bikel, Lukas Blecher, Cristian Canton Ferrer, Moya Chen, Guillem Cucurull, David Esiobu, Jude Fernandes, Jeremy Fu, Wenyin Fu, Brian Fuller, Cynthia Gao, Vedanuj Goswami, Naman Goyal, Anthony S. Hartshorn, Saghar Hosseini, Rui Hou, Hakan Inan, Marcin Kardas, Viktor Kerkez, Madian Khabsa, Isabel M. Kloumann, Artem Korenev, Punit Singh Koura, Marie-Anne Lachaux, Thibaut Lavril, Jenya Lee, Diana Liskovich, Yinghai Lu, Yuning Mao, Xavier Martinet, Todor Mihaylov, Pushkar Mishra, Igor Molybog, Yixin Nie, Andrew Poulton, Jeremy Reizenstein, Rashi Rungta, Kalyan Saladi, Alan Schelten, Ruan Silva, Eric Michael Smith, R. Subramanian, Xia Tan, Binh Tang, Ross Taylor, Adina Williams, Jian Xiang Kuan, Puxin Xu, Zhengxu Yan, Iliyan Zarov, Yuchen Zhang, Angela Fan, Melissa Hall Melanie Kambadur, Sharan Narang, Aurélien Rodriguez, Robert Stojnic, Sergey Edunov, and Thomas Scialom. Llama 2: Open foundation and fine-tuned chat models. *ArXiv*, abs/2307.09288, 2023. URL <https://api.semanticscholar.org/CorpusID:259950998>.
- [30] Alex Wang, Yada Pruksachatkun, Nikita Nangia, Amanpreet Singh, Julian Michael, Felix Hill, Omer Levy, and Samuel R. Bowman. Superglue: A stickier benchmark for general-purpose language understanding systems. *ArXiv*, abs/1905.00537, 2019. URL <https://api.semanticscholar.org/CorpusID:143424870>.
- [31] Wei Wen, Chunpeng Wu, Yandan Wang, Yiran Chen, and Hai Helen Li. Learning structured sparsity in deep neural networks. In *Neural Information Processing Systems*, 2016. URL <https://api.semanticscholar.org/CorpusID:2056019>.
- [32] Peng Xu, Wenqi Shao, Mengzhao Chen, Shitao Tang, Kai-Chuang Zhang, Peng Gao, Fengwei An, Yu Qiao, and Ping Luo. Besa: Pruning large language models with block-wise parameter-efficient sparsity allocation. *ArXiv*, abs/2402.16880, 2024. URL <https://api.semanticscholar.org/CorpusID:268032346>.
- [33] An Yang, Anfeng Li, Baosong Yang, Beichen Zhang, Binyuan Hui, Bo Zheng, Bowen Yu, Chang Gao, Chengen Huang, Chenxu Lv, Chujie Zheng, Dayiheng Liu, Fan Zhou, Fei Huang, Feng Hu, Hao Ge, Haoran Wei, Huan Lin, Jialong Tang, Jian Yang, Jianhong Tu, Jianwei Zhang, Jianxin Yang, Jiaxin Yang, Jingren Zhou, Jingren Zhou, Junyan Lin, Kai Dang, Keqin Bao, Ke-Pei Yang, Le Yu, Li-Chun Deng, Mei Li, Min Xue, Mingze Li, Pei Zhang, Peng Wang, Qin Zhu, Rui Men, Ruize Gao, Shi-Qiang Liu, Shuang Luo, Tianhao Li, Tianyi Tang, Wenbiao Yin, Xingzhang Ren, Xinyu Wang, Xinyu Zhang, Xuancheng Ren, Yang Fan, Yang Su, Yi-Chao Zhang, Yinger Zhang, Yu Wan, Yuqiong Liu, Zekun Wang, Zeyu Cui, Zhenru Zhang, Zhipeng Zhou, and Zihan Qiu. Qwen3 technical report. 2025. URL <https://api.semanticscholar.org/CorpusID:278602855>.
- [34] Lu Yin, You Wu, Zhenyu (Allen) Zhang, Cheng-Yu Hsieh, Yaqing Wang, Yiling Jia, Mykola Pechenizkiy, Yi Liang, Zhangyang Wang, and Shiwei Liu. Outlier weighed layerwise sparsity (owl): A missing secret sauce for pruning llms to high sparsity. *ArXiv*, abs/2310.05175, 2023. URL <https://api.semanticscholar.org/CorpusID:263829692>.
- [35] Rowan Zellers, Ari Holtzman, Yonatan Bisk, Ali Farhadi, and Yejin Choi. Hellaswag: Can a machine really finish your sentence? In *Annual Meeting of the Association for Computational Linguistics*, 2019. URL <https://api.semanticscholar.org/CorpusID:159041722>.
- [36] Susan Zhang, Stephen Roller, Naman Goyal, Mikel Artetxe, Moya Chen, Shuohui Chen, Christopher Dewan, Mona T. Diab, Xian Li, Xi Victoria Lin, Todor Mihaylov, Myle Ott, Sam Shleifer, Kurt Shuster, Daniel Simig, Punit Singh Koura, Anjali Sridhar, Tianlu Wang, and Luke Zettlemoyer. Opt: Open pre-trained transformer language models. *ArXiv*, abs/2205.01068, 2022. URL <https://api.semanticscholar.org/CorpusID:248496292>.

A Detailed Cross-Model Results Under 2:4 Sparsity

For readability, the main text reports a compact cross-model summary using mean zero-shot accuracy only. In this appendix, we provide the full task-level results corresponding to the cross-model comparison in Table 1. Table 4 reports the dense-model performance, SparseForge performance, and their differences on each benchmark under 2:4 semi-structured sparsity, together with the mean accuracy and WikiText-2 perplexity.

Table 4: Detailed cross-model results under 2:4 semi-structured sparsity. We report zero-shot accuracy (%) on downstream tasks, the mean accuracy across tasks, and WikiText-2 perplexity (PPL) for the dense model, SparseForge, and their differences.

Model	Variant	ARC-c	ARC-e	BoolQ	Hella.	OBQA	RTE	Wino.	Mean	Wiki PPL
GPT-2-Medium	Dense	21.67	49.07	58.41	33.23	18.60	52.71	53.12	40.97	21.80
	SparseForge	21.16	46.04	60.09	31.70	16.40	53.43	53.35	40.31	25.90
	Diff	-0.51	-3.03	+1.68	-1.53	-2.20	+0.72	+0.24	-0.66	+4.10
GPT-2-Large	Dense	21.84	53.16	60.55	36.39	19.40	52.71	55.25	42.76	18.95
	SparseForge	22.10	50.29	61.90	34.68	19.40	52.71	53.59	42.10	23.57
	Diff	+0.26	-2.86	+1.35	-1.70	+0.00	+0.00	-1.66	-0.66	+4.62
GPT-2-XL	Dense	25.09	58.29	61.68	40.00	22.60	52.35	58.41	45.49	17.12
	SparseForge	23.29	55.98	61.77	38.37	21.40	54.15	55.41	44.34	20.53
	Diff	-1.79	-2.31	+0.09	-1.63	-1.20	+1.81	-3.00	-1.15	+3.41
OPT-2.7B	Dense	26.79	60.77	60.40	45.86	25.00	54.51	61.01	47.76	12.45
	SparseForge	25.17	58.67	63.06	44.44	21.80	52.71	60.85	46.67	15.14
	Diff	-1.62	-2.10	+2.66	-1.41	-3.20	-1.81	-0.16	-1.09	+2.69
Qwen3-1.7B	Dense	39.85	72.26	77.58	46.09	28.20	70.76	60.85	56.51	15.56
	SparseForge	37.97	70.08	74.53	46.30	27.00	56.68	60.77	53.33	10.54
	Diff	-1.88	-2.19	-3.06	+0.21	-1.20	-14.08	-0.08	-3.18	-5.02
Qwen3-8B	Dense	55.80	83.50	86.61	57.14	31.00	78.34	67.72	65.73	8.97
	SparseForge	50.85	81.52	82.35	54.34	31.60	72.92	69.30	63.31	8.03
	Diff	-4.95	-1.98	-4.25	-2.80	+0.60	-5.42	+1.58	-2.42	-0.94
Qwen3-14B	Dense	58.45	84.18	89.33	60.96	35.00	77.62	73.01	68.36	7.89
	SparseForge	53.67	82.24	84.92	57.94	34.40	72.20	72.69	65.44	7.17
	Diff	-4.78	-1.94	-4.40	-3.03	-0.60	-5.42	-0.32	-2.93	-0.72
DeepSeek-MoE	Dense	45.05	75.88	72.72	58.09	32.00	62.82	70.24	59.54	6.28
	SparseForge	41.47	74.12	73.82	57.45	32.00	62.09	69.06	58.57	6.92
	Diff	-3.58	-1.77	+1.10	-0.64	+0.00	-0.72	-1.18	-0.97	+0.64

B Extension to Block-16 Sparsity

Although our main experiments focus on the practically important 2:4 semi-structured pattern, the SparseForge formulation is not inherently restricted to this setting. In particular, the score-based projection and progressive quenching mechanism can be adapted to other structured sparsity patterns by redefining the feasible group and projection operator. To examine this generality, we additionally evaluate SparseForge under a block-16 sparsity pattern. Concretely, in our block-16 setting, each 16×16 weight block is constrained to contain only 50% nonzero entries. Compared with 2:4 sparsity, this is a relatively looser form of structured sparsity: the sparsity pattern is still constrained at the block level, but the competition among weights is imposed over a larger local region rather than by a strict fine-grained $n:m$ rule within every group of four.

Table 5 reports results on several representative model families under block-16 sparsity. Overall, SparseForge remains effective beyond 2:4, with moderate degradation on most model families and benchmarks. In particular, LLaMA-2-7B retains strong performance under block-16, with mean accuracy dropping from 59.70% to 59.02% (a 0.68-point decrease). OPT-2.7B remains nearly unchanged, showing a slight mean improvement from 47.76% to 47.93%. Similar trends are also observed on GPT-2-XL, where the mean accuracy only decreases from 45.49% to 45.14%.

At the same time, the block-16 setting appears to be more challenging for some architectures, especially smaller or more sensitive models. For example, Qwen3-1.7B shows a larger drop in mean accuracy (from 56.47% to 53.49%), and DeepSeek-MoE-16B also exhibits a noticeable decrease (from 59.54% to 58.20%). These results suggest that while the proposed mask optimization strategy

transfers beyond 2:4, the degree of recoverability under block-structured sparsity still depends on model architecture and training dynamics.

Overall, these results support the view that SparseForge is a general mask optimization framework rather than a method tied specifically to 2:4 sparsity. We leave a more systematic study of different structured sparsity patterns and their hardware-accuracy

Table 5: SparseForge under block-16 sparsity across model families. We report mean zero-shot accuracy before and after sparsification.

Model	Base Mean	Block-16 Mean	Diff
LLaMA-2-7B	59.70	59.02	-0.68
OPT-2.7B	47.76	47.93	+0.17
GPT-2	37.13	37.58	+0.45
GPT-2-Medium	41.01	39.45	-1.56
GPT-2-Large	42.65	41.87	-0.81
GPT-2-XL	45.49	45.14	-0.35
Qwen3-1.7B	56.47	53.49	-2.98
DeepSeek-MoE-16B	59.54	58.20	-1.34

Table 6: Detailed results of SparseForge under block-16 sparsity on LLaMA-2-7B.

Variant	ARC-c	ARC-e	BoolQ	Hella.	OBQA	RTE	Wino.	Mean
Dense	43.43	76.26	77.71	57.17	31.40	62.82	69.14	59.70
SparseForge	41.89	75.25	76.24	56.78	32.20	61.73	69.06	59.02
Diff	-1.54	-1.01	-1.47	-0.39	+0.80	-1.08	-0.08	-0.68

C End-to-End Inference Speedup

Table 7: End-to-end inference throughput (tokens/s) of SparseForge 2:4 sparse LLaMA-2-7B vs. dense baseline, measured with TensorRT-LLM on an NVIDIA H800 GPU under different input/output sequence lengths. The last row reports the model weight memory footprint. “Efficiency” denotes the sparse-over-dense ratio (speedup for throughput, compression ratio for memory).

(Inp Len, Out Len)	Sparse	Dense	Efficiency
(128, 128)	108.72	75.41	1.44×
(128, 1024)	106.18	74.63	1.42×
(1024, 128)	103.87	73.62	1.41×
(1024, 1024)	101.29	72.38	1.40×
Memory Consumption	7.31 GB	12.55 GB	0.58×

Beyond accuracy recovery, a practical motivation for adopting the 2:4 semi-structured pattern is that it is directly supported by modern NVIDIA sparse Tensor Cores [22], enabling tangible end-to-end acceleration on real hardware. To verify that our SparseForge-trained 2:4 sparse models translate into actual deployment gains, we evaluate their inference throughput using TensorRT-LLM¹ on an NVIDIA H800 GPU, under four different input/output sequence length settings. We use the 2:4 sparse LLaMA-2-7B model produced by SparseForge, and compare its decoding throughput (tokens/s) and memory footprint against the corresponding dense model under identical inference configurations.

Table 7 reports the results. Across all input/output length configurations, the 2:4 sparse model consistently outperforms its dense counterpart, delivering 1.40×–1.44× throughput improvements on H800. In addition, the memory footprint of model weights is reduced to roughly 58% of the dense baseline (7.31 GB vs. 12.55 GB for LLaMA-2-7B), which directly lowers the GPU memory

¹<https://github.com/NVIDIA/TensorRT-LLM>

requirement for deployment. Together with the accuracy results in the main text, these measurements confirm that SparseForge produces 2:4 sparse models that are not only competitive in quality but also practically deployable, converting the algorithmic sparsity gain into measurable end-to-end latency and memory savings on commodity inference hardware.

D Discussion and Limitations

Scaling retraining tokens is not the only path. Recent semi-structured sparsification work largely treats closing the gap to the dense model as a matter of *how many tokens* one is willing to spend on retraining. Our results push back on this implicit assumption: on LLaMA-2-7B under 2:4 sparsity, SparseForge matches the strongest retraining-based baseline (CAST[†]) while using roughly an order of magnitude fewer retraining tokens (Table 2, Figure 5), and this efficiency does not come at the cost of generality—the same recipe preserves model quality across architectures ranging from GPT-2 variants to 14B dense Qwen3 and a 16B MoE model (Table 1). The ablations in §5.4 further show that the gain cannot be attributed to a single trick: removing Hessian-aware importance, the SLoRB branch, or structure-aware signal each causes a clear drop, indicating that making the mask a first-class optimization variable, scoring it with curvature-aware signals, and annealing it into the deployable pattern address complementary failure modes of semi-structured sparse recovery. This does not argue against retraining at scale; rather, it suggests that *where* optimization effort is spent matters at least as much as how long it runs, and that better mask optimization is a more efficient lever than additional tokens for pushing semi-structured sparse models toward dense-level quality.

Limitations. Our results remain sensitive to the choice of retraining corpus: the larger degradation observed on Qwen3 in Table 1 is most plausibly explained by the mismatch between its reasoning-oriented pretraining mixture and the generic C4 data we use for recovery, and a stronger task-aligned corpus would likely narrow this gap. We also focus primarily on 2:4 sparsity—with only a preliminary block-16 study in Appendix B—on a fixed set of model families.